DEVELOPMENTAL BIOLOGY **181,** 79–90 (1997)
ARTICLE NO. DB968447

Analysis of Cell Movement and Signalling during Ring Formation in an Activated Gα1 Mutant of *Dictyostelium discoideum* That Is Defective in Prestalk Zone Formation

Jens Rietdorf, Florian Siegert, Suranganie Dharmawardhane,* Richard A. Firtel,* and Cornelis J. Weijer†,[1]

*Zoologisches Institut, Universität München, Luisenstrasse 14, 80333 Munich, Germany; †Department of Anatomy & Physiology, Old Medical School, University of Dundee, DD1 4HN Dundee, United Kingdom; and *Department of Biology, Center for Molecular Genetics, University of California at San Diego, La Jolla, California 92093-0634*

Mound formation in the cellular slime mould *Dictyostelium* results from the chemotactic aggregation of competent cells. Periodic cAMP signals propagate as multiarmed spiral waves and coordinate the movement of the cells. In the late aggregate stage the cells differentiate into prespore and several prestalk cell types. Prestalk cells sort out chemotactically to form the tip, which then controls all further development. The tip organises cell movement via a scroll wave that converts to planar waves in the prespore zone leading to rotational cell movement in the tip and periodic forward movement in the prespore zone. Expression of an activated Gα1 protein under its own promoter leads to a severely altered morphogenesis from the mound stage onwards. Instead of forming a tipped mound, the cells form a ring-shaped structure without tip. Wave propagation pattern and dynamics during aggregation and mound formation in the mutant are indistinguishable from the parental strain AX3. However, at the time of tip formation the spiral waves that organise the late aggregate do not evolve in a scroll-organising centre in the tip but transform into a circularly closed (twisted) scroll ring wave. This leads to the formation of a doughnut-shaped aggregate. During further development, the doughnut increases in diameter and the twisted scroll wave converts into a train of planar waves, resulting in periodic rotational cell movement. Although biochemical consequences resulting from this mutation are still unclear, it must affect prestalk cell differentiation. The mutant produces the normal proportion of prespore cells but is unable to form functional prestalk cells, i.e., prestalk cells with an ability to sort out from the prespore cells and form a prestalk zone. Failure of sorting leads to an altered signal geometry, ring-shaped scroll waves, that then directs ring formation. This mutant demonstrates the importance of prestalk cell sorting for the stabilisation of the scroll wave that organises the tip.

INTRODUCTION

Early aggregation of the slime mould *Dictyostelium* is driven by periodic waves of cAMP that instruct the cells to collect at the aggregation centre. Recent experiments show that coordinated cell movement in slugs and mounds is due to the same mechanisms that operate during early aggregation, i.e., cAMP relay and chemotaxis (Siegert and Weijer, 1992, 1995; Bretschneider *et al.*, 1995). We developed a theory that states that all of *Dictyostelium* morphogenesis up to the culmination stage is organised by periodic waves and chemotactic movement (Rietdorf *et al.*, 1996; Siegert and Weijer, 1995). Furthermore, we proposed that the geometry of the waves is a major determinant of the type of mound and slug morphogenesis. This has already been shown for the aggregation stage of *Dictyostelium* development (Siegert and Weijer, 1989; Höfer *et al.*, 1995; Vasiev *et al.*, 1994; Lee *et al.*, 1996). This theory needs to be tested by investigation of morphogenesis after perturbation of the signal-response system in signal transduction and motility mutants. In earlier studies, we have described an altered morphogenesis resulting from inhibition of the activation of adenylyl cyclase (Siegert and Weijer, 1989). Inhibition of

[1] To whom correspondence should be addressed. Fax: 0044-13482-345514. E-mail: c.j.weijer@dundee.ac.uk. http://www.zi.biologie.uni-muenchen.de/zoologie/dicty/dicty.html.

0012-1606/97 $25.00

adenylyl cyclase activation by caffeine resulted in a less efficient relay and therefore in an increase in oscillation period. This increase in period length led to an increase in signal wavelength and therefore in an increase in the diameter of the spiral core, resulting in ring-shaped aggregation centres. However, caffeine primarily affects calcium homeostasis and therefore may affect multiple processes including the cell motility system. One of the advantages of the *Dictyostelium* system is that many components of the cAMP signalling system have been cloned and that mutants in these components can now be generated by gene replacement with mutated forms. This allows one to create more defined disturbances in cAMP signalling and/or chemotaxis pathways.

The molecular basis for cAMP relay during early aggregation is well characterised and involves the $G\alpha_2$ and $G\beta\gamma$ subunits of heterotrimeric G-proteins, the seven-helix transmembrane cAMP receptor CAR1, an adenylyl cyclase (ACA), and CRAC, a plecstrin homology domain containing protein involved in the activation of adenylyl cyclase (Kumagai *et al.*, 1991; Sun and Devreotes, 1991; Johnson *et al.*, 1992; Pitt *et al.*, 1992; Pupillo *et al.*, 1992; Devreotes, 1994; Lilly and Devreotes, 1995; Wu *et al.*, 1995). In total, eight developmentally regulated $G\alpha$-subunits of heterotrimeric G-proteins have been identified in *Dictyostelium*. $G\alpha_2$ and $G\alpha_4$ are involved in the signal transduction cascades of the chemoattractants cAMP and folate, respectively (Devreotes, 1994; Hadwiger *et al.*, 1994; Firtel, 1995). The signal transduction cascades in which the other $G\alpha$ proteins play a role are still largely unknown.

Mutants of $G\alpha_1$(G45V), which are defective in GTP hydrolysis and therefore in a continuous activated state, show an aberrant morphological development at the mound stage. Aggregation is normal and mounds are formed, but then they then open up to form ring-shaped aggregates, which transform to slugs very inefficiently and only after a significant delay. After more than 70 hr of development, they form small fruiting bodies with a thick base. Furthermore they show a reduced production of cAMP in response to cAMP pulses (Dharmawardhane *et al.*, 1994). To investigate the link between this altered morphogenesis and cell signalling, we monitored several parameters relevant to the signalling system such as the geometry of the dark-field waves, wave propagation speed and frequency, cell movement, as well as cellular differentiation *in vivo*. Cells expressing $G\alpha_1$(G45V) were indistinguishable from wild-type AX3 until the early mound stage. In the mound the proportioning into prespore and prestalk cells is normal; however, the prestalk cells do not sort out correctly from the prespore cells. Failure of cell sorting leads to a different spatial geometry of the cAMP signal. The spiral waves usually found in wild-type mounds convert to a circularly closed scroll wave giving rise to the formation of a ring of cells instead of tipped aggregates.

MATERIALS AND METHODS

Strains, culture, and developmental conditions. AX3 cells were grown axenically in HL5 medium as described by Sussmann (1987). The cells were grown to a density of $1-6 \times 10^6$ cells/ml and harvested by low speed centrifugation. To initiate development cells were placed at density of 5×10^5 cells/cm^2 on 1% KK2 (20 m*M* potassium phosphate, pH 6.8) agar plates and incubated at 22°C for 6–12 hr. Usually aggregation started at 6 hr of development, tipped mounds formed after 12 hr. Neutral red staining was performed as described in Weijer *et al.* (1987).

The percentage of prespore cells was determined as the number of cells expressing the prespore-specific cell surface protein PSA, detected by indirect immunofluorescence staining with the monoclonal antibody MUD1 as described in Bichler and Weijer (1994). The construction and biochemical characterisation of the $G\alpha$1(G45V mutant is described in Dharmawardhane *et al.* (1994). The cells were grown in HL5 medium in the presence of 20 μg/ml G418. AX3–actin15–GFP (A15GFP) cells were also grown in HL5 containing 20 μg/ml G418. Fluorescent AX3 cells were obtained by transforming AX-3 cells with a construct containing the gene for GFP (green fluorescent protein; Chalfie *et al.*, 1994) under the control of the *Dictyostelium* actin-15 promoter. Shortly, the GFP fragment was cut from the DdGFP vector generously provided by R. Kay (Cambridge) as a *Bam*HI–*Xho*I fragment and inserted in a PB15 vector (provided by D. Mannstein, London) where GFP is expressed under the control of an actin-15 (A15) promoter. For synergy experiments the cells were harvested at densities between 2 and 8×10^6/ml, collected by low speed centrifugation, and washed two times in KK2 buffer. A15GFP cells (0.5% of the sample) were mixed with the mutant $G\alpha$1(G45V) and plated onto 1% KK2 agar at a density of 5×10^7/plate. The plates were incubated in the dark for various times at 22°C.

Measurement of dark-field wave propagation. Dark-field wave propagation was observed under oblique illumination using a Zeiss IM 35 inverted microscope equipped with 2.5× or 6.3× objectives. The illumination was adjusted by shifting the phase ring partly in the light path in such a way that the faint optical density signals related to cell shape changes were enhanced maximally. These optical density waves became visible only in time-lapse recordings. The dark-field waves were recorded with a Hamamatsu C-2400-08 SIT camera adjusted to medium high sensitivity in order to reduce the light intensity. The video signal was analogue adjusted to obtain high contrast and then digitised by a video frame grabber board (AFG; Imaging Technology) which allows real-time averaging of incoming video frames. To enhance image quality usually 32 frames were averaged and the resulting image was saved to a laser video disk (Sony LVR 4000) in time-lapse mode every 5–20 sec. Time–space plots were generated and analysed as described in Siegert and Weijer (1989, 1995).

Cell movement analysis of GFP-labelled cells. To determine the movement of individual cells in aggregates and mounds we mixed a low percentage (0.1–0.5%) of fluorescent GFP-expressing AX3 cells with unlabelled $G\alpha$1(G45V) cells (Hodgkinson, 1995; Fey *et al.*, 1995; Rietdorf *et al.*, 1996). Fluorescence was observed in a Zeiss inverted microscope (Axiovert 10) equipped with special filters (short pass 425DF45, dichroic mirror 475 nm, long pass 450 nm; Omega Optical Instruments S.A., Grasbrunn, Germany). The cells were observed with 20× or 40× Neofluar objectives. The excitation light was reduced 64-fold by neutral density filters in order to avoid damage of the cells. Video images were recorded with a Hamamatsu C-2400-08 SIT camera adjusted to maximal sensitivity. To further reduce the exposure of the cells to damaging illumination the exposure time was reduced to 0.6 sec every 5 sec using a computer-controlled shutter. Within these 0.6 sec 16 video frames were averaged and stored as described above. This technique allowed us to track GFP-labelled cells for more than 2.5 hr without

any noticeable photo damage of the cells. For movement analysis the cells were tracked either automatically or interactively on screen as described in Siegert and Weijer (1991, 1992) using specially written application programs.

Synergy experiments. Synergy experiments between the mutant and the wild-type cells were performed by mixing 5% fluorescently labelled mutant cells with wild-type cells and allowing them to form slugs on petri dishes containing 1% water agar. The cells were labelled by incubating them for 30 min at 22°C in 100 μM cell tracker green (Molecular Probes; 1:100 dilution from 10 mM stock in DMSO) in KK2 buffer. Finally the cells were washed twice and mixed with wild-type cells.

RESULTS

Morphological comparison of AX3 and Gα1(G45V) mounds. A direct comparison of the development of the activated Gα1 mutant G45V and the wild-type strain AX3 shows a dramatically altered morphogenesis from the mound stage onwards (Fig. 1). The left side of Fig. 1 shows development of the activated Gα1 mutant G45V (Figs. 1A–1D) taken at successive time points. The corresponding stages of the wild-type strain are shown at the right (Figs. 1E–1H). No differences in morphology can be observed until 10 hr of starvation (Figs. 1A, 1B, 1E, and 1F). The different numbers of arms seen in Figs. 1A and 1E are within the natural variation of each strain. However, after 12 hr of development, mutant mounds started to flatten centrally and became irregular in shape, while wild-type mounds became hemispheric. During the next 2 hr (12–14 hr), the central depression in Gα1 mutants enlarged until a ring-shaped aggregate formed. During the same time, a tip formed in wild-type aggregates (Figs. 1C and 1G). After 14–16 hr of starvation, the wild-type mound elongated and a first finger formed, while in the mutant the ring continuously widened (Figs. 1D and 1H). The mutant cells continued to migrate in a loop for more than 48 hr. Eventually the rings broke up and a slug formed producing a small thick-based fruiting body after more than 70 hr of starvation. The wild type usually completed development after 24 hr. These data show that the most prominent feature of the Gα1(G45V) mutant is its inability to form a functional tip.

Signal propagation in the Gα1(G45V) mutant. In a previous study, we characterised the evolution of signalling and cell movement during mound formation in the wild type (Rietdorf *et al.,* 1996). We found drastic changes in signalling parameters as well as in cell movement during mound formation. These changes correlated with important events such as cellular differentiation and cell sorting. We supposed that the altered morphogenesis in the mutant might result from alterations in the control of cell movement. In order to investigate if a defect in cAMP signal relay is responsible for the observed phenotype, we analysed dark-field wave propagation. Dark-field waves are directly correlated to the cAMP relay response, since they reflect the chemotactic response of the cells (Tomchik and Devreotes, 1981). In a previous study, we showed that the Gα1(G45V) mutant has a strongly reduced cAMP relay response as well as a decreased cAMP-stimulated cGMP response (Dharmawardhane *et al.,* 1994).

Ring-shaped aggregation centres could be caused by a weak relay response leading to an increase in period length and chemical wave length. Previously, we observed loop-shaped aggregation when cells were plated in the presence of caffeine, a known inhibitor of adenylyl cyclase activation (Brenner and Thoms, 1984), leading to a significant slow-down of the optical density wave oscillations and an increase in wave length (Gross *et al.,* 1976; Siegert and Weijer, 1989). To test this hypothesis, we measured several signalling parameters like wave period and wave propagation speed as well as cell movement characteristics.

The late aggregation stage and early mound stage (with still incoming streams) of both the wild-type and the mutant were organised by multiarmed spiral waves (Rietdorf *et al.,* 1996). The number of spiral arms varied between 2 and 10. We observed up to 20 rotations of these waves. Then followed a period when no wave propagation could be observed. The reason for this was that in the wild type, the tip was forming, while the mutant exhibited an altered geometry of the signal that caused the cells to rotate vertically instead of horizontally (see below). During this time, mutant mounds opened up and formed ring-shaped structures (Fig. 2). In such rings (Fig. 2C), dark-field waves could be observed in time-lapse movies. To visualise the faint differences in light scattering caused by moving and not moving cells we subtracted successive video images, a technique that amplifies these differences in optical density (Siegert and Weijer, 1995; Lee *et al.,* 1996). (Figs. 2B and 2D). Each pair of black and white bands in Figs. 2B and 2D represents just one wavelength of a moving optical density wave caused by active cell movement in response to a cAMP wave (Siegert and Weijer, 1995). Figures 2A and 2C show the corresponding dark-field video images. As in the case of multiarmed spirals, there exists more than one wave front in these rings. As the rings increased in size, additional wave fronts appeared (compare Figs. 2B and 2D).

To study the dynamics of wave propagation over time and in more detail, we constructed time–space plots. An example of such a time–space plot for a ring of the mutant G45V is given in Figs. 3A and 3B. Light scattering signals of dark-field waves are seen as diagonally downward-oriented lines going from left to right in the time–space plot (Fig. 3B). The slope of these lines reflects signal propagation velocity. From the spacing between successive bands the period of the dark-field waves can be directly determined. There are also signals going in an opposite direction pointing diagonally downward from the upper right to the lower left. These lines are less pronounced and less regular as the dark-field waves. These bands reflect cell movement. They consist of many fine parallel lines, which represent moving intracellular structures like small vesicles. The larger dark regions are shadows that are caused by the local accumulation of cells leading to a local thickening of the ring. The slope of these lines reflects the rate of cell movement in a direction opposite to the direction of wave propagation.

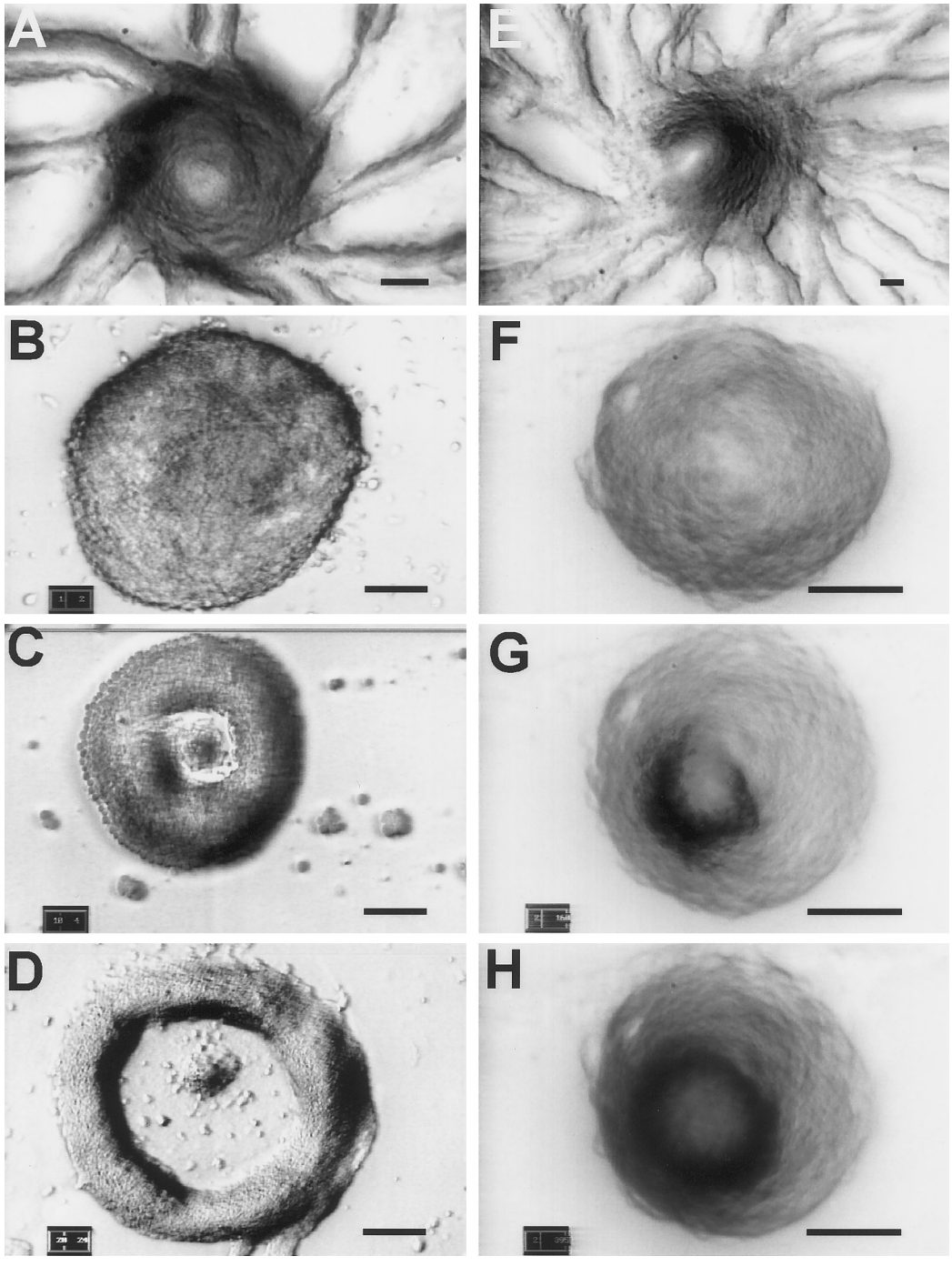

FIG. 1. Developmental stages of the Gα1 mutant G45V (A–D) and the parent strain AX3 (E–H). Development of the mutant Gα1(G45V) at 8 (A), 10 (B), 12 (C), and 14 (D) hr of development. Development of the parent strain AX3 at 8 (E), 10 (F), 12 (G), and 14 (H) hr of development. Scale bar, 50 μm.

This enabled us to measure both the signal velocity and the cell movement velocity simultaneously.

Between 24 and 36 hr of development, the average oscillation period in rings increased from 4 to 8 min (Fig. 3C, solid line). Compared to the parental strain AX3 the period is nearly twice as long. The propagation speed for dark-field waves was low throughout this period (30–100 μm/min; see Table 1) and showed values similar to those found in the wild-type mounds. Average cell movement velocity was almost as high as the wave propagation velocity and stayed

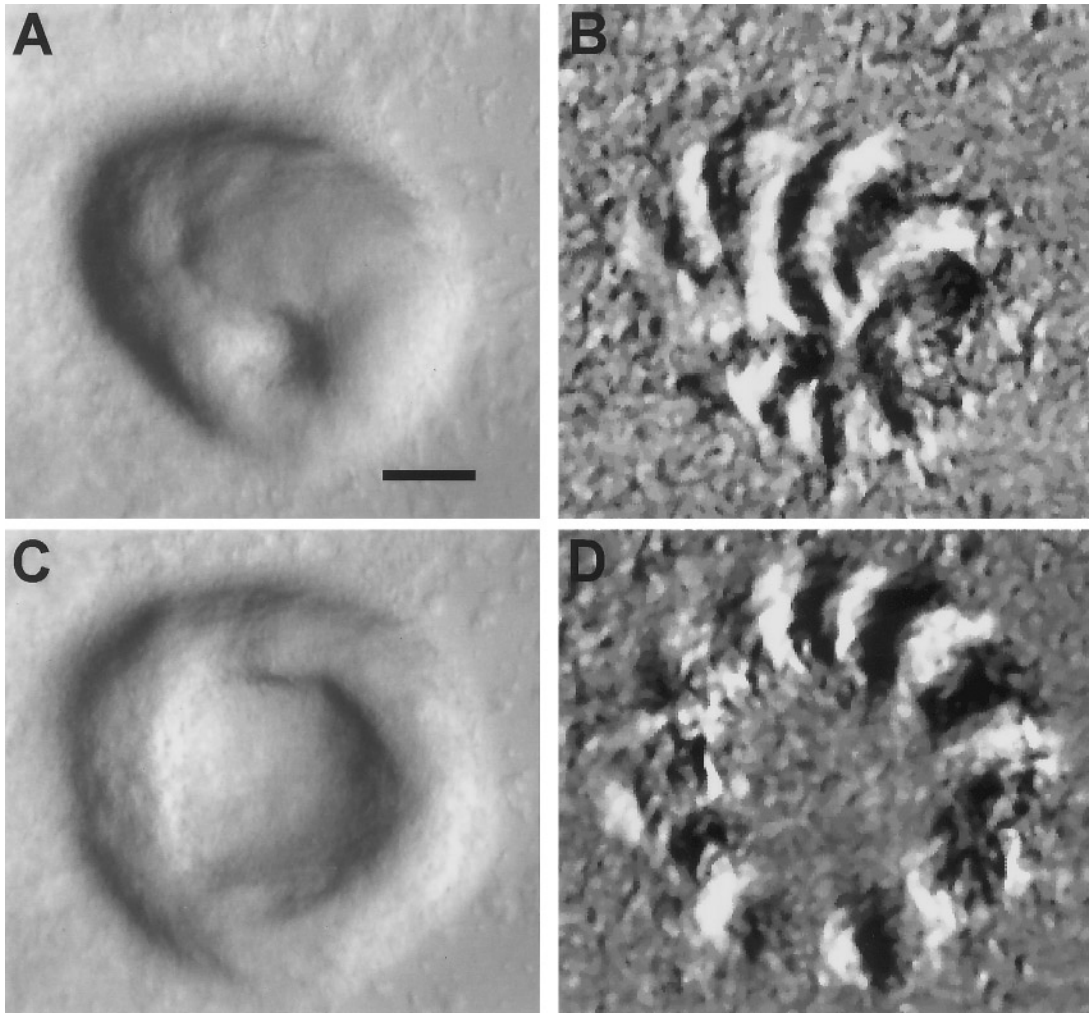

FIG. 2. Subtraction images showing multiple waves in rings of G45V. (A) Transmitted light image of ring which just starts to open. (B) Optical density waves as visualised by the successive method. (C) Transmitted light image of the same ring 2 hr later when it opened up further. (D) Waves visualised in the ring shown in C.

constant with values ranging from 30 to 80 μm/min (Table 1). These values were considerably higher than those found in the wild-type mounds and slugs. The measurements of the wave period are made with respect to the substratum. Cell movement speed is nearly as fast as the wave propagation speed and since the waves propagate in a direction opposite to the direction of cell movement, this will lead to a Doppler effect. The apparent period of the cAMP waves experienced by the cells will be considerably shorter than that measured with respect to the substratum. The apparent period, as calculated from the experimental data, is shown in Fig. 3C (dotted line) and is considerable lower as measured from dark-field waves. It decreased from 2 to 4 min between 24 and 36 hr of development, which compares favourably with the period obtained from direct cell tracking experiments in mounds (Rietdorf *et al.*, 1996).

The measurements indicate relatively constant periods of 2–3 min for the perceived signals during all of later *Dictyostelium* development. This implies that the different cAMP receptors that appear during development and that most likely mediate these signals must have similar adaptation–deadaptation kinetics with half-times of 2–3 min as measured for the CAR1 receptor (Dinauer *et al.*, 1980).

There are no correlations between development time and wave velocity or cell movement speed in rings. However, there is a significant negative correlation between wave propagation velocity and the number of waves per ring (Fig. 3D). The more waves are propagating in a ring the slower the wave propagation velocity in agreement with the dispersive properties of the signalling system (Gross *et al.*, 1976; Siegert and Weijer, 1989, 1991; Keener, 1980; Keener and Tyson, 1986).

Cell movement in the Gα1(G45V) mutant. In order to observe how rings form as a result of altered cell movement,

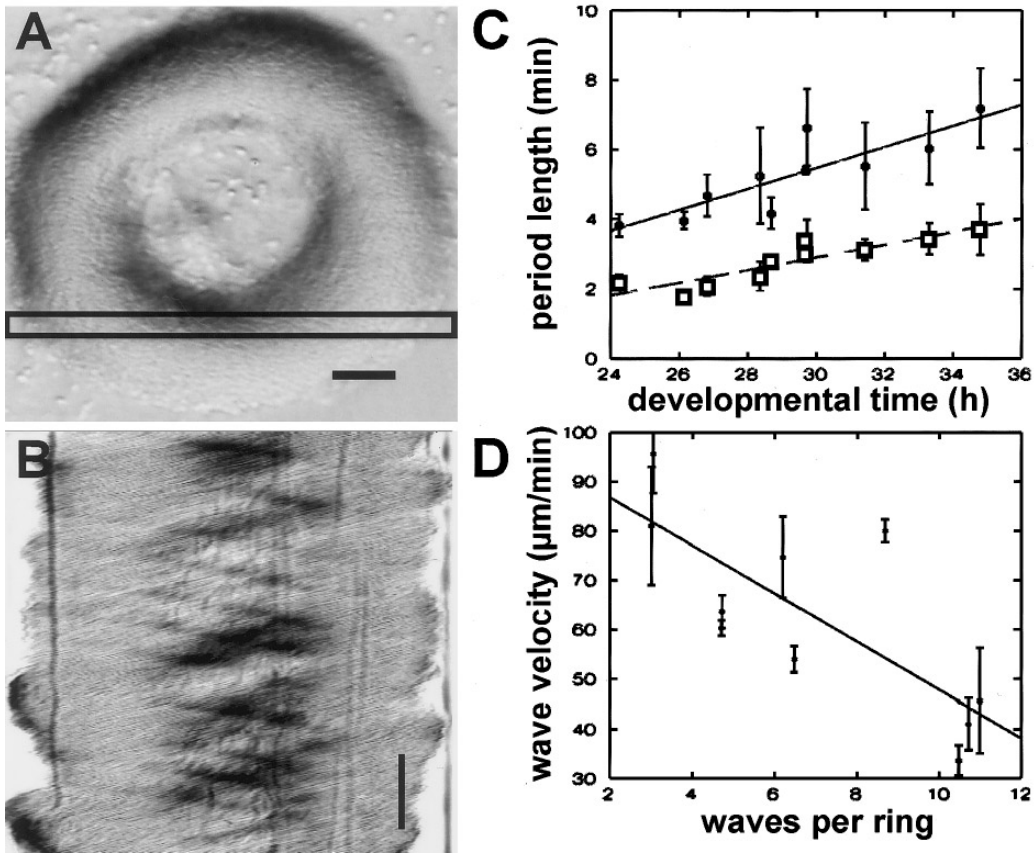

FIG. 3. Time–space plot analysis of wave propagation and cell movement in G45V rings. (A) Phase contrast image of a G45V ring after 20 hr of development. The scale bar is 100 μm. The open window indicates the area used to calculate the time–space plot. (B) Time–space plot measured over a period of 2 hr in a ring at 20 hr of development. The time–space plot is generated by measuring the grey level (averaged over the height of the window to reduce noise) along the long axis of the window placed over one side of the ring (A) and displaying a sequence of successive grey level distributions, taken at 10-sec intervals, from the top to the bottom. (C) Dependence of period of wave period as measured (solid line) and the calculated period experienced by the cells (dotted line) as a function of developmental age. (D) Number of waves plotted as a function of ring diameter. There is a clear negative correlation (slope is -0.79, which is highly significant; $P < 0.05$ in a nonparametric test).

we analysed cell movement of individual labelled cells by mixing 0.1–0.5% of A15/GFP cells with Gα1(G45V) mutant cells. The AX3 cells were used as indicators for the signals produced by the mutant host. We traced cell movement in all stages of development and found that up to the late aggregate stage there were no detectable differences in the behaviour of these cells in a wild-type or G45V environment. The cells moved in aggregation streams with speeds which were statistically not different from those measured in wild-type cells, implying that there are no major differences in signal relay parameters. The cells were elongated and underwent periodic changes in cell shape typical for cells in aggregation streams. As they entered the mound, they slowed down considerably as in wild-type mounds and their movement trajectories were irregular (Fig. 4A). Figure 4B shows a schematic drawing of the signals coordinating cell movement at this stage. The first detectable differences between mutant and wild type appeared just before the rings began to form. The mutant cells changed their movement pattern to scrolling trajectories of an inverse fountain type as can be seen in Fig. 4C. The tracked cell moved from the upper periphery of the mound towards the centre where it dived down towards the bottom of the mound and then moved back again at the lower side towards the periphery. It could be tracked manually for a long period although it periodically appeared and disappeared from the plane of focus. The cell apparently follows the trajectory of a twisted scroll whose filament is oriented parallel to the substrate. This movement is most likely coordinated by a counter rotating twisted scroll wave of cAMP. Figure 4D shows a schematic drawing of a scroll ring wave organising inverse fountain cell movement. For simplicity the scroll is not twisted. During inverted fountain movement a depression formed in the middle of the mound (Figs. 1C and 2A). Later the central depression deepened in mutant mounds and ring-shaped structures formed (Fig. 2C) in which the cells

TABLE 1

Wave Propagation and Cell Movement Parameters Measured in Rings of the G45V Mutant between 25 and 35 hr of Development

Development time (hr)	Period (min)	Wave velocity (μm/min)	Cell velocity (μm/min)	Diameter of ring (μm)	Calculated period (min)	Waves per ring
24	3.8 ± 0.3	74.7 ± 8.2	55.6 ± 4.5	570	2.2 ± 0.2	6
26	4.0 ± 0.3	45.7 ± 10.6	57.0 ± 3.6	630	1.8 ± 0.2	11
27	4.7 ± 0.6	54.0 ± 2.6	67.1 ± 3.5	520	2.1 ± 0.3	7
28	5.3 ± 1.4	41.0 ± 5.2	50.0 ± 11.9	730	2.4 ± 0.4	11
29	4.2 ± 0.4	80.0 ± 2.3	38.9 ± 6.7	920	2.8 ± 0.1	9
30	5.4 ± 0.1	95.7 ± 8.0	75.3 ± 7.4	500	3.0 ± 0.1	3
30	6.6 ± 1.1	33.7 ± 3.1	32.3 ± 2.5	740	3.4 ± 0.6	11
31	5.5 ± 1.3	60.3 ± 1.6	46.2 ± 4.9	500	3.1 ± 0.3	5
33	6.0 ± 1.0	63.7 ± 3.3	48.0 ± 4.5	580	3.4 ± 0.4	5
35	7.2 ± 1.1	81.0 ± 12.0	75.9 ± 6.9	560	3.7 ± 0.7	3

Note. The data represent the means and standard errors of the means of 3–9 successive waves measured in a particular ring at the time indicated. From these values the signal period experienced by the cells and the number of waves per ring were calculated. The subjective period experienced by the cells (P_c) due to fast movement of the cells in direction opposite to the light scattering signals is given by

$$P_c = P_w\,(V_w/(V_w + V_c)), \qquad [1]$$

where P_w is the signal period length as determined from the time–space plots, V_c the velocity of the cells, and V_w the velocity of the signal. From the period and the wave propagation velocity it is possible to calculate the chemical wavelength and therefore the number of waves per ring N given as

$$N = \Pi x\, D_r/(V_{wx}P_w), \qquad [2]$$

where D_r is the diameter of the ring, V_w the velocity of the signal, and P_w the signal period, It is seen that the subjective period increases slightly during development. Furthermore there is no clear correlation between ring size and number of waves per ring.

followed simple ring-shaped trajectories at high speeds (Fig. 4E). The corresponding signals are planar wavefronts, as can be seen from subtraction images (Figs. 4F and 2D). Sometimes we also found cells moving along twisted scroll trajectories. The speed measured by tracking individual A15/GFP cells (49.4 ± 14.8 μm/min, $N = 50$) in rings is directly comparable with the average cell speed derived for the time–space plots using Gα1(G45V) cells (Table 1, column 4). This shows that AX3 cells are good indicators for G45V movement behaviour.

A summary of the changes in speed during development measured by single cell tracking is given in Fig. 5. In the wild-type strain AX3 there exist two different control points were parameters for cell behaviour are changing abruptly during mound formation. In the early mound stage after about 7 hr of starvation, the time when the cells enter the mound, cell movement speed first decreases and then increases later to reach its highest value at about 12 hr (solid line). This is exactly the time when tip formation starts. During cell sorting, movement slows down again and becomes clearly periodic shortly before extension of the first finger (Rietdorf *et al.*, 1996). The cell movement velocity profile for the mutant looks similar to that seen in the wild-type strain AX3 until 10 hr of development. Afterwards, there is a clear difference; while there is sharp increase in cell movement in the wild type, it increases only slightly in the mutant (dotted line). After many hours of development, cell movement speed of the mutant finally reaches high values similar to those observed in AX3 just before tip formation.

Prespore–prestalk differentiation in Gα1(G45V) mutants. The phenotype of the mutant is that it does not form tips. Moreover, Gα1 may be involved in prestalk cell differentiation since overexpression of Gα1 under its own promoter leads to a failure of differentiation of the pstAB cells in the core of the slug tip (Dharmawardhane *et al.*, 1994). We therefore decided to investigate cell-type proportioning in the G45V mutant. We used the vital dye neutral red to stain specifically the prestalk and anterior-like cell population. In wild-type mounds the majority of the neutral red-stained prestalk cells sort out to form the tip. However, a small proportion of neutral red-stained cells (approx 10%), termed anterior-like cells, stays intermingled with prespore cells. These cells do not sort out from prespore cells unless the tip is decapitated (Sternfeld and David, 1981, 1982). In the mutant, we observed many neutral red-stained cells with big autophagic vacuoles; however, these neutral red-stained cells in the rings did not sort out (Fig. 6A). Most of the neutral red-stained cells remained dispersed randomly in the midst of unstained cells. Sometimes a small proportion of neutral red-stained cells accumulated in the inner periphery of the rings. Interestingly, in almost all rings ob-

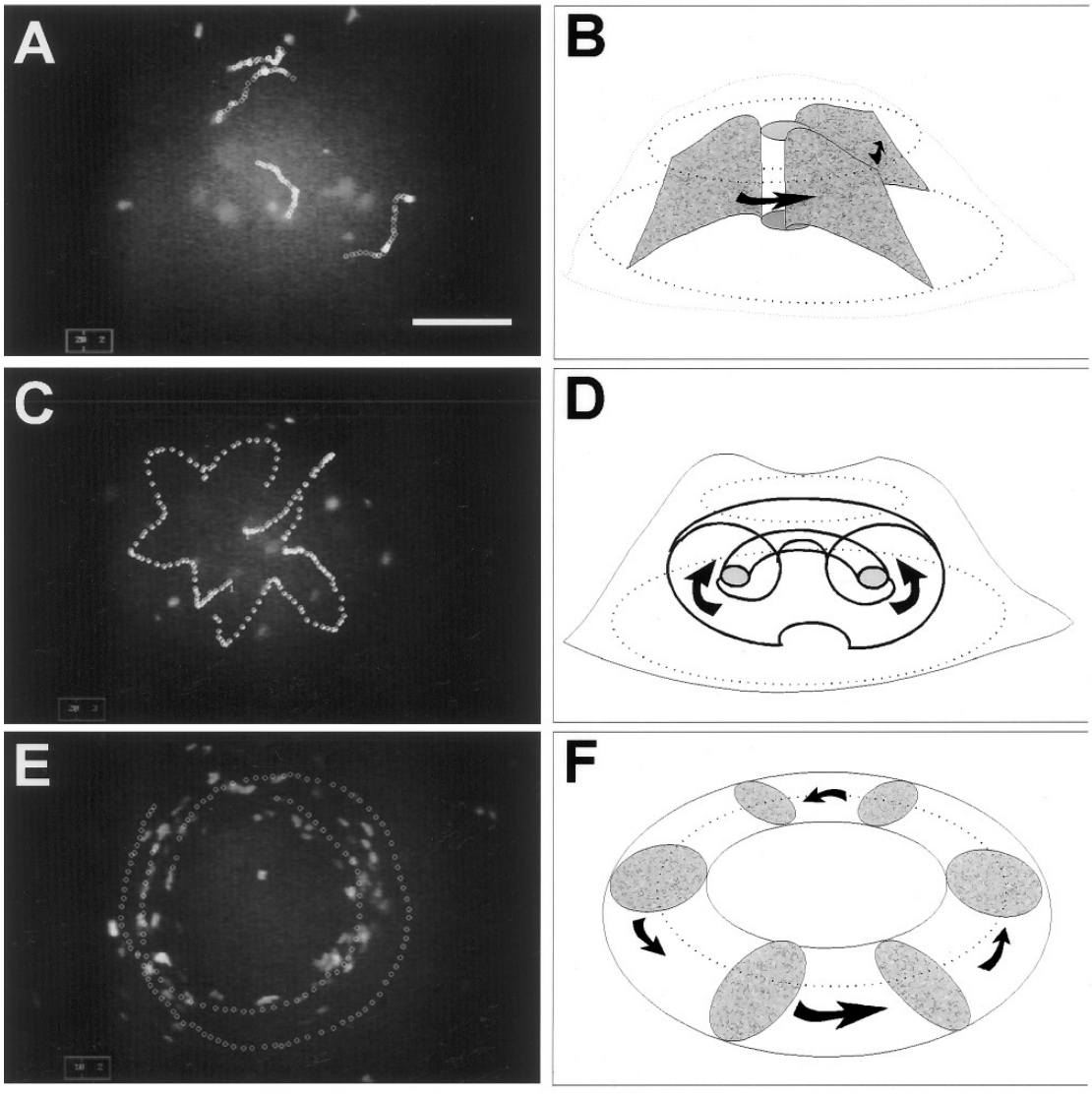

FIG. 4. Cell movement of A15GFP cells in mounds and rings of the mutant G45V during successive stages of ring development. (A) Movement tracks of four GFP-expressing cells measured over a period of 1000 sec. (B) Schematic drawing of the signals directing the movement of the cells during the time the movement was recorded in A. (C) Tracks of two cells describing twisted scroll movement trajectories during the initial stages of ring formation. (D) Twisted scroll wave signal responsible for the movement observed in C. (E) Simple rotational movement in older rings (20 hr of development). Cells were followed for 1000 sec. (F) Series of planar waves in a ring responsible for the cell movement pattern observed in E.

served, a group of very intensely neutral red-stained cells formed a pile in the middle of the ring (see Fig. 6A).

To investigate prespore–prestalk cell proportioning quantitatively, we determined the kinetics of the number of cells expressing the prespore-specific antigen PSA during development in mutant and parental wild-type strains. Both the timing and the proportion of cells expressing the prespore-specific cell surface protein PSA were indistinguishable from wild-type (Fig. 6B), showing that they both form a normal proportion of prespore cells. The other cells, which do not differentiate into prespore cells, enter the prestalk pathway, deduced from the observation that they stain heavily with neutral red. These cells are anterior-like cells since they do not sort out from the prespore cells to make a tip (Sternfeld and David, 1981), suggesting that the Gα1(G45V) mutant is defective in the proportioning of prestalk and anterior-like cell types.

To test this hypothesis we performed sorting experiments in which we investigated the differentiation preference of the mutant in competition with wild-type cells. As can be seen in Fig. 6C, 5% of the labelled mutant cells sort to positions normally occupied by pst0/anterior-like cells. The

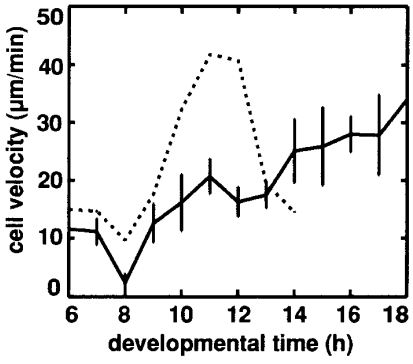

FIG. 5. Dynamics of cell movement during development of G45V. The movement data of G45V (solid line) shows that the movement of the cells in G45V mounds slows down for a short period at 8 hr of development and then steadily increases. For comparison the dynamics of AX3 movement are indicated as a dotted line.

mutant cells are clearly excluded from the tip, suggesting that they are defective in prestalk A cell differentiation.

DISCUSSION

The formation of rings is caused by the transition of spiral waves to twisted scroll rings. The Gα1(G45V) mutant expresses an activated Gα1 protein under the control of its own promoter in a *gα1*-null background. This mutant aggregates normally and forms a mound but, instead of developing a tip, mounds of this mutant form a depression in the centre and evolve into ring-shaped aggregates (Figs. 1A–1D). These ring structures persist for a long period of time (up to 72 hr) and can increase and decrease in diameter repeatedly. Analysis of the patterns of wave propagation and cell movement in this mutant showed that the signals from early aggregation up to the early mound stage are indistinguishable from the parent strain AX3 (Rietdorf *et al.*, 1996; G45V data not shown). Although it was shown by Dharmawardhane (1994) that the cAMP-induced cAMP production is decreased 4- to 5-fold, we do not expect this to influence the appearance of the optical density waves. We have shown previously that the optical density waves are in the presence of 2 m*M* caffeine are not very different from wild-type waves (Siegert and Weijer, 1989) although the cAMP relay response is reduced more than 20-fold in 2 m*M* caffeine (Brenner and Thoms, 1984). This shows that optical density wave propagation can occur over a wide range of relay parameters. During early aggregation the waves propagate as single-armed spirals that increase in frequency and then convert into multiarmed spirals at the mound stage. Wave propagation speed also decreases as seen in the wild type, and average cell movement speed gradually reaches values found during the fast rotation phase in wild-type mounds, just before tip formation (Fig. 5). This implies that the alterations observed in cAMP relay and cGMP production measured at the early aggregation stage (Dharmawardhane *et al.*, 1994) have no major phenotypic consequences.

The most striking change in the signalling parameters observed in the mutant is a change in the geometry of the

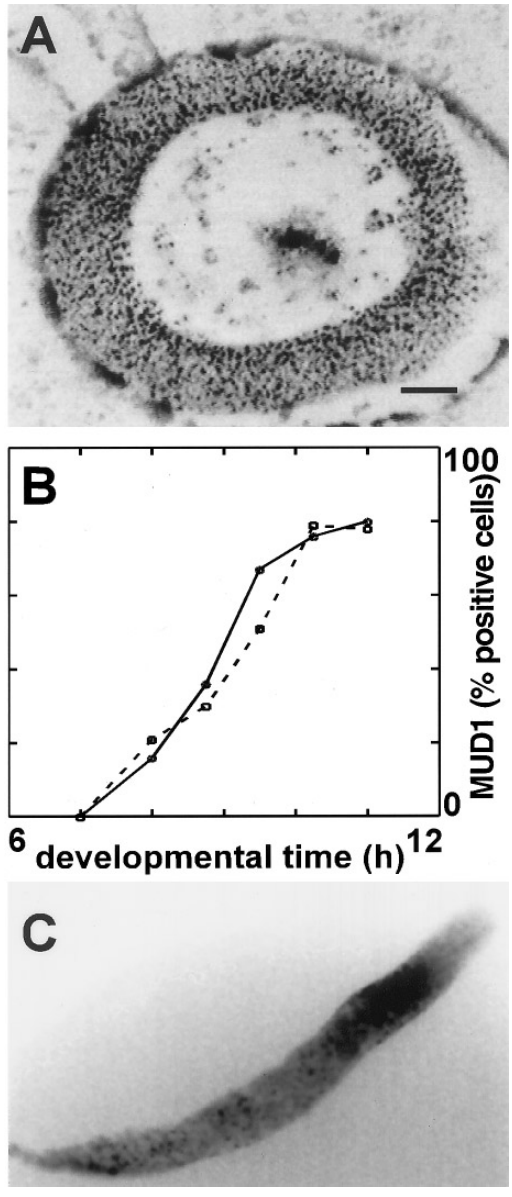

FIG. 6. Prespore and prestalk differentiation in the mutant G45V. (A) G45V ring at 20 hr of development after staining of the cells with neutral red. The neutral red-stained cells are visible as black dots and preferentially located in the inner sector of the ring. Bar, 50 μm. (B) Time course of PSA-expressing cells of the mutant G45V (solid line) and the parent strain AX3 (broken line). The percentage of PSA-expressing cells was determined as the number of MUD1-positive cells. (C) AX3 slug containing 5% cell tracker green-labelled G45V cells. Labelled cells, shown in black, are excluded from the tip and accumulate in the pst0 region. The tip points to the upper right corner.

darkfield waves. While wild-type mounds are organised by multiarmed spirals that convert to a scroll wave in the tip, the multiarmed spirals found in early mutant mounds transform into scroll rings during ring formation and finally into a train of planar waves. In other words, the mutant is unable to establish a scroll wave organiser as is typical for wild-type strains.

During the stage of the multiarmed spirals, the filament of these spirals (the core of the spiral, drawn as a cylinder in Figs. 4B and 4D) is located in the centre of the mound and extends from the top to the bottom of the mound (Fig. 4B). In the wild type, the prestalk cells will now sort out and form the tip and in the process of doing so stabilise the scroll wave in the tip that converts to planar waves in the body of the mound, which consists of prespore and anterior-like cells (Siegert and Weijer, 1992; Bretschneider *et al.*, 1995). In the mutant, the cells do not sort and, during the formation of the rings, the cells start to move along inverse fountain-like trajectories, which we think are organised by scroll rings as indicated in Figs. 4C and 4D. In this case, the axis of the filament is oriented parallel to the substrate. Often these scroll rings are twisted along the horizontal axis of the filament as suggested by the cell track in Fig. 4C.

Based on our observations and the theory of excitable media, it can be understood how the rings increase in size. Once a twisted scroll ring is formed and the filament is closed on itself (circular), there is no limitation to the length of the filament. Since the waves are spiral shaped, there is a net inward movement directed towards the central filament of the scroll ring, i.e., all cells try to move towards the centre. This can only be accomplished if the ring increases in diameter. If the rings widen and become thinner and thinner, the scroll presumably starts to twist and finally breaks, giving rise to a series of successive planar waves propagating through the rings (Figs. 4E and 4F).

An unsolved problem is how the initially straight and vertically oriented filament in the multiarmed spirals gives rise to a circular filament in the twisted scroll rings. This requires that the filament detaches from the upper and lower surface of the mound and the free ends start to drift and eventually join up to form a circular closed filament. One possible hypothesis might be that the filament disconnects from the bottom because differentiated cells in the centre of the ring accumulate at the bottom and are no longer excitable (see below). They may then form a nonexcitable region which forces the filament to detach and move sideways. Alternatively, it might be that rings are the final stable situation in a three-dimensional excitable medium that does not show an intrinsic gradient in excitability as generated in the wild type by cell sorting.

Ring formation has also been observed in mixtures of NC4 and AX3 cells (Clark *et al.*, 1980). Although it has not been investigated why and how these rings arise, it has been proposed that the circumference of these rings is exactly one chemical wavelength, a so-called PV loop (Clark and Steck, 1979). From our experiments, it is evident that this simple relationship does not hold since we found regularly multiple wavefronts in a ring (Fig. 2D). If the rings widened, new waves arose and the number of planar wavefronts travelling in rings increased. We found a strong negative correlation between the number of waves per ring and the propagation velocity of the waves (Fig. 3D). This reflects the dispersive properties of an excitable medium, i.e., cAMP waves propagate slower if the cells do not have sufficient time to fully resensitise between successive waves (Siegert and Weijer, 1989).

Ring-shaped aggregation centres are also formed if wild-type cells are placed on agar containing 5 m*M* caffeine. Caffeine is a strong inhibitor of cAMP relay and the diameter of the rings is correlated to the amount of caffeine applied (Brenner and Thoms, 1984; Siegert and Weijer, 1989). The reduced relay response leads to an increase in period length and therefore to an increase of the diameter of the spiral core. However, there are fundamental differences to the rings observed in the Gα1(G45V) mutant. While the mutants form rings first from the mound stage onwards and continue to rotate for many hours, rings treated with caffeine break up to form many small, but normal-shaped mounds. Below 3 m*M* caffeine the rings collapse again and form a mound, a property we never observed in Gα1(G45V) mutants.

The Gα1(G45V) mutant is defective in tip formation, suggesting a defect in prestalk–anterior-like cell proportioning. Since we found that cell movement and signalling were normal during mound formation but that the Gα1(G45V) mutant does not form tips, we expect that the mutation might affect prespore–prestalk differentiation. In order to assess the differentiation state of the cells at the ring stage of development, we investigated the expression of the prespore-specific protein PSA (Goolley *et al.*, 1990). Cells expressing the prespore antigen PSA arise with normal kinetics and in normal proportions (80% of all cells) already at the streaming aggregate stage (Fig. 6B). This is indistinguishable from the parent strain AX3 and shows that the cell-type proportioning into the prestalk and prespore pathways is normal. Neutral red staining of the G45V cells showed that, from the late mound stage onwards, many cells show the prestalk and anterior-like cell-specific staining of autophagic vacuoles. However, these cells do not sort out from the unstained prespore cells but stay randomly intermingled with prespore cells and therefore functionally behave as anterior-like cells (Fig. 6A). At the moment it is still very difficult to test for defects in anterior-like/prestalk cell proportioning since there are as yet no good molecular markers that are only expressed in anterior-like cells or only in tip cells. The synergy experiments between Gα1(G45V) and the parental strain AX3 showed that the mutant cells were excluded from the tip and accumulated in the pst0 region. Since pst0 cells and anterior-like cells have been shown to form an interchanging population (Abe *et al.*, 1994), this finding is compatible with a defect in prestalk (tip cell) differentiation of mutant cells.

The phenotype of the G45V mutant can readily be explained by a defect in prestalk to anterior-like cell proportioning leading to the absence of functional prestalk cells

(no tip-forming capacity). The mutant lacks cells that sort out from prespore cells and set up a tip as the new organising centre. Therefore, these mounds do not differentiate into slugs with a prestalk–prespore zone but differentiate into ''prespore-like pieces'' consisting of prespore and anterior-like cells. The rings can be viewed as circularly closed prespore zones that are organised by series of waves propagating around the ring, which do not need an organiser (tip) since they are self-sustaining.

Although the molecular basis for the effect of the Gα1(G45V) mutation remains still unclear, these experiments suggest that Gα1(G45V) mutation interferes with the decision to differentiate into anterior-like or prestalk cells. The studies with Gα1 promoter β-galactosidase reporter constructs have shown that the Gα1 gene is expressed in specific subclasses of prestalk cells, anterior-like cells, and cells that are found in the core of the slug tip (Dharmawardhane *et al.,* 1994). This expression pattern is very similar to the pstPST B expression pattern (Williams and Morrison, 1994). Overexpression of the Gα1 wild-type protein under control of its own promoter leads to the disappearance of ecmAB cells in the central core of the slug while ecmB expression is still present in anterior-like cells in the prespore zone (Dharmawardhane *et al.,* 1994). These mutants are still able to form slugs, implying that the loss of ecmB-expressing cells in the core of the tip is not sufficient to inhibit tip formation. The G45V mutant shows a much stronger phenotype than the Gα1 overexpresser: it does not succeed very efficiently in forming slugs. From our experiments, it seems likely that overexpression of the G45V mutation under the control of the Gα1 promoter will block the formation of ''tip cells.'' At this stage tip cells are defined by their property to sort out from prespore cells.

Cell sorting most likely involves a chemotactic mechanism and although the molecular basis for cell sorting is still unsolved, it seems that isolated prestalk cells show a more vigorous chemotactic movement than anterior-like and prespore cells (Early *et al.*, 1995). This might possibly be based on expression of different subsets of cAMP receptors, allowing the cells to react differently to cAMP (Yu and Saxe, 1995) or, alternatively, it might be due to developmentally regulated and cell-type-specific changes in the cytoskeleton (Springer *et al.*, 1994). Furthermore, cell-type-specific differences in cell adhesion might play a role. Our present experiments cannot discriminate between the possibility that the primary defect in the mutant is actually caused by a defect in anterior-like–prestalk cell proportioning, leading to a lack of tip cell function or whether the defect in tip formation is caused by a specific inhibition of any of the above-mentioned processes involved in prestalk cell sorting.

Ring formation could be an indicator of a defect in prestalk function. Scroll rings and inverse fountain cell movement in mounds have been described before by Durston and Vork (1979). They observed the occasional formation of these structures on growth plates of the wild-type strain NC4 in the presence of very high concentrations of the dye neutral red. Neutral red is a weak base and selectively accumulates and discharges acidic compartments in the cells. Therefore, it might be expected that high concentrations of neutral red will affect prestalk cells more strongly than other cells since they posses the largest autophagic vacuoles. At high concentrations. the prestalk cells might be severely disabled or even killed, while leaving prespore and possibly anterior-like cells relatively unaffected. Therefore, we consider it likely that the mechanism of ring formation on neutral red plates is similar to that in the G45V mutant described here and that ring formation might be a good indicator of a defect in the prestalk function.

ACKNOWLEDGMENTS

We thank the Deutsche Forschungsgemeinschaft (We 1127) for financial support. This work was supported in part by USPHS Grants GM24279 and GM37830 to R.A.F.

REFERENCES

Abe, T., Early, A., Siegert, F., Weijer, C., and Williams, J. (1994). Patterns of cell movement within the *Dictyostelium* slug revealed by cell type-specific, surface labellinglabeling of living cells. *Cell* **77,** 687–699.

Bichler, G., and Weijer, C. J. (1994). A *Dictyostelium* anterior-like cell mutant reveals sequential steps in the prespore prestalk differentiation pathway. *Development* **120,** 2857–2868.

Brenner, M., and Thoms, S. D. (1984). Caffeine blocks activation of cyclic AMP synthesis in *Dictyostelium discoideum*. *Dev. Biol.* **101,** 136–146.

Bretschneider, T., Siegert, F., and Weijer, C. J. (1995). Three-dimensional scroll waves of cAMP could direct cell movement and gene expression in *Dictyostelium* slugs. *Proc. Natl. Acad. Sci. USA* **92,** 4387–4391.

Chalfie, M., Tu, Y., Euskirchen, G., Ward, W. W., and Prasher, D. C. (1994). Green fluorescent protein as a marker for gene expression. *Science* **263,** 802–805.

Clark, R. L., and Steck, T. L. (1979). Morphogenesis in *Dictyostelium:* An orbital hypothesis. *Science* **204,** 1163–1168.

Clark, R. L., Retzinger, G. S., and Steck, T. L. (1980). Novel morphogenesis in Ax-3, a mutant strain of the cellular slime mould *Dictyostelium discoideum*. *J. Gen. Microbiol.* **121,** 319–331.

Devreotes, P. N. (1994). G protein-linked signalling pathways control the developmental program of *Dictyostelium*. *Neuron* **12,** 235–241.

Dharmawardhane, S., Cubitt, A. B., Clark, A. M., and Firtel, R. A. (1994). Regulatory role of the g alpha 1 subunit in controlling cellular morphogenesis in *Dictyostelium*. *Development* **120,** 3549–3561.

Dinauer, M. C., Steck, T. L., and Devreotes, P. N. (1980). Cyclic 3′,5′-AMP relay in *Dictyostelium* discoideum. V. Adaptation of the cAMP signalling response during cAMP stimulation. *J. Cell Biol.* **86,** 554–561.

Durston, A. J., and Vork, F. (1979). A cinamatographical study of the development of vitally stained *Dictyostelium discoideum*. *J. Cell Sci.* **36,** 261–279.

Early, A., Abe, T., and Williams, J. (1995). Evidence for positional differentiation of prestalk cells and for a morphogenetic gradient in *Dictyostelium*. *Cell* **83,** 91–99.

Fey, P., Compton, K., and Cox, E. C. (1995). Green fluorescent protein production in the cellular slime molds *Polysphondylium pallidum* and *Dictyostelium discoideum*. *Gene* **165,** 127–130.

Firtel, R. A. (1995). Integration of signaling information in controlling cell-fate decisions in *Dictyostelium*. *Gene Dev.* **9,** 1427–1444.

Gooley, A. A., Ti, Z. C., Bernstein, R. L., Smith, E., and Williams, K. L. (1990). Identification and purification of the cell surface glycoprotein homologous to psA in different species of cellular slime mold on the basis of a shared carbohydrate epitope. *Dev. Genet.* **11,** 484–491.

Gross, J. D., Peacey, M. J., and Trevan, D. J. (1976). Signal emission and signal propagation during early aggregation in *Dictyostelium discoideum*. *J. Cell Sci.* **22,** 645–656.

Hadwiger, J. A., Lee, S., and Firtel, R. A. (1994). The g(alpha) subunit g(alpha)4 couples to pterin receptors and identifies a signaling pathway that is essential for multicellular development in *Dictyostelium*. *Proc. Natl. Acad. Sci. USA* **91,** 10566–105709.

Hodgkinson, S. (1995). GFP in *Dictyostelium*. *Trends Genet.* **11,** 327–328.

Hofer, T., Sherratt, J. A., and Maini, P. K. (1995). *Dictyostelium discoideum:* Cellular self-organization in an excitable biological medium. *Proc. R. Soc. London Biol.* **259,** 249–257.

Johnson, R. L., Gunderson, R., Hereld, D., Pitt, G. S., Tugendreich, S., Saxe, C. L., III, Kimmel, A. R., and Devreotes, P. N. (1992). G-protein linked signaling pathways mediate development in *Dictyostelium*. *Cold Spring Harbor Symp. Quant. Biol.* **57,** 169–176.

Keener, J. P. (1980). Waves in excitable media. *SIAM J. Appl. Math.* **39,** 528–548.

Keener, J. P., and Tyson, J. J. (1986). Spiral waves in the Belousoc Zhabotinsky reaction. *Physica D* **21,** 307–324.

Kumagai, A., Hadwiger, J. A., Pupillo, M., and Firtel, R. A. (1991). Molecular genetic analysis of two G(alpha) protein subunits in *Dictyostelium*. *J. Biol. Chem.* **266,** 1220–1228.

Lee, K. L., Cox, E. C., and Goldstein, R. E. (1996). Competing patterns of signalling activity in *Dictyostelium discoideum*. *Phys. Rev. Lett.* **76,** 1174–1177.

Lilly, P. J., and Devreotes, P. N. (1995). Chemoattractant and GTP gamma S-mediated stimulation of adenylyl cyclase in *Dictyostelium* requires translocation of CRAC to membranes. *J. Cell Biol.* **129,** 1659–1665.

McRobbie, S. J., Jermyn, K. A., Duffy, K., Blight, K., and Williams, J. G. (1988). Two DIF-inducible, prestalk-specific mRNAs of *Dictyostelium* encode extracellular matrix protein of the slug. *Development* **104,** 275–284.

Pitt, G. S., Milona, N., Borleis, J., Lin, K. C., Reed, R. R., and Devreotes, P. N. (1992). Structurally distinct and stage-specific adenylyl cyclase genes play different roles in *Dictyostelium* development. *Cell* **69,** 305–315.

Pupillo, M., Insall, R., Pitt, G. S., and Devreotes, P. N. (1992). Multiple cyclic AMP receptors are linked to adenylyl cyclase in *Dictyostelium*. *Mol. Biol. Cell* **3,** 1229–1234.

Rietdorf, J., Siegert F., and Weijer, C. J. (1995). Analysis of optical density wave propagation and cell movement during mound formation in *Dictyostelium discoideum*. *Dev. Biol.* **177,** 427–438.

Siegert, F., and Weijer, C. (1989). Digital image processing of optical density wave propagation in *Dictyostelium discoideum* and analysis of the effects of caffeine and ammonia. *J. Cell Sci.* **93,** 325–335.

Siegert, F., and Weijer, C. J. (1991). Analysis of optical density wave propagation and cell movement in the cellular slime mould *Dictyostelium discoideum*. *Physica D* **49,** 224–232.

Siegert, F., and Weijer, C. J. (1992). Three-dimensional scroll waves organize *Dictyostelium* slugs. *Proc. Natl. Acad. Sci. USA* **89,** 6433–6437.

Siegert, F., and Weijer, C. J. (1995). Spiral and concentric waves organize multicellular *Dictyostelium* mounds. *Curr. Biol.* **5,** 937–943.

Springer, M. L., Patterson, B., and Spudich, J. A. (1994). Stage-specific requirement for myosin II during dictyostelium development. *Development* **120,** 2651–2660.

Sternfeld, J., and David, C. N. (1981). Cell sorting during pattern formation in *Dictyostelium*. *Differentiation* **20,** 10–21.

Sternfeld, J., and David, C. N. (1982). Fate and regulation of anterior-like cells in *Dictyostelium* slugs. *Dev. Biol.* **93,** 111–118.

Sun, T. J., and Devreotes, P. N. (1991). Gene targeting of the aggregation stage cAMP receptor cAR1 in *Dictyostelium*. *Genes Dev.* **5,** 572–582.

Tomchik, K., and Devreotes, P. (1981). Adenosine 3′:5′-monophosphate waves in *Dictyostelium discoideum:* A demonstration by isotope dilution-fluorography. *Science* **212,** 443–446.

Vasiev, B., Hogeweg, P., and Panfilov, A. (1994). Simulation of *Dictyostelium discoideum* aggragation via reaction–diffusion model. *Phys. Rev. Lett.* **73,** 3173–3176.

Williams, J., and Morrison, A. (1994). Prestalk cell-differentiation and movement during the morphogenesis of *Dictyostelium discoideum*. *Prog. Nucleic Acid Res. Mol. Biol.* **47,** 1–27.

Weijer, C. J., David, C. N., and Sternfeld, J. (1987). Vital staining methods used in the analysis of cell sorting in *Dictyostelium discoideum*. *Methods Cell Biol.* **28,** 449–459.

Wu, L. J., Valkema, R., Vanhaastert, P. J. M., and Devreotes, P. N. (1995). The G protein beta subunit is essential for multiple responses to chemoattractants in *Dictyostelium*. *J. Cell Biol.* **129,** 1667–1675.

Yu, Y., and Saxe, C. L., III (1995). Differential distribution of cAMP receptors cAR2 and cAR3 during *Dictyostelium* development. *Dev. Biol.* **173,** 353–356.

Received for publication July 26, 1996
Accepted October 15, 1996